Template-Based Growth of Various Oxide Nanorods by Sol–Gel Electrophoresis**

By *Steven J. Limmer*, *Seana Seraji*, *Yun Wu*, *Tammy P. Chou*, *Carolyn Nguyen*, and *Guozhong Cao**

The ability to form oxide nanorods is of great interest in a number of areas. In this paper, we report the template-based growth of nanorods of several oxide ceramics, formed by means of a combination of sol–gel processing and electrophoretic deposition. Both single metal oxides (TiO_2, SiO_2) and complex oxides ($BaTiO_3$, $Sr_2Nb_2O_7$, and $Pb(Zr_{0.52}Ti_{0.48})O_3$) have been grown by this method. Uniformly sized nanorods of about 125–200 nm in diameter and 10 μm in length were grown over large areas with near unidirectional alignment. Desired stoichiometric chemical composition and crystal structure of the oxide nanorods was readily achieved by an appropriate procedure of sol preparation, with a heat treatment (700 °C for 15 min) for crystallization and densification.

1. Introduction

In recent years, one of the most active areas of research has been nanotechnology. Besides the general drive towards miniaturization (as in the microelectronics industry), nanosized materials are interesting for the new range of physics that they allow one to study. For example, quantum dots of CdSe show size-dependence in several of their properties, such as photoluminescence.[1] They also have the potential for many interesting applications. For example, the high surface area of TiO_2 nanorods has been demonstrated to yield far better photocatalytic behavior than bulk TiO_2 films.[2] In addition, analysis of the properties and features of nanosized structures necessarily requires the development of techniques for reliably forming nanostructures.

Various growth techniques have been studied for the formation of nanorods and nanowires. For example, nanorods of Si have been grown by a vapor–liquid–solid (VLS) method,[3] in which a gaseous Si source (e.g., $SiCl_4$) diffuses into a drop of molten Si–Au alloy, causing Si to nucleate and grow from the droplet. A variant of this technique using laser ablation (laser-assisted catalytic growth, LAC) has been used to form nanorods of compound semiconductors.[4] A third example is the solution-based growth of Se nanowires.[5] Thermal evaporation of oxide powders has been demonstrated as a means of forming ribbon-like nanostructures of various oxides.[6]

Another common fabrication method for nanostructures such as rods, wires, and hollow tubules is the template-based synthesis technique. In this method, a porous membrane (such as radiation track-etched polycarbonate, PC, or anodic alumina) is used as a template for growing the desired materials. Since the porous membranes are easily fabricated (or commercially available) with a large range of possible pore diameters, this provides a simple technique for making nanorods with the desired diameter. This technique has been widely used to form numerous materials, including metal and polymer nanorods,[2,7–9] oxide nanorods,[2,7,10,11] and composite nanostructures.[2,12] For metal and conducting polymer rods grown with a template, the method generally used is electrochemical deposition. The template is placed in contact with the electrode where the metal (or polymer) is being deposited, and the pores of the template are filled. This electrochemical method can also serve as the first step in growth of oxide nanorods, where an electrochemically grown metal wire is oxidized by heating in air to form a metal oxide rod.[11]

Another method used for the formation of oxide rods is direct sol filling, in which a sol of the desired oxide material is allowed to infiltrate the pores of the template. As an example, Martin and co-workers have succeeded in forming TiO_2 wires with this technique.[2,10] However, there are some potential disadvantages to this technique. For instance, capillary action drawing the sol into the template is the only driving force forming nanorods from the sol. In addition, sols commonly have a low solids content (~5 vol.-%). Thus, even if the pores are filled with sol, the packing of solids in the pores is very low. Increasing the concentration of the sol could partially alleviate this difficulty, but using too high a concentration could either result in a sol so viscous that filling of the pores would be difficult, or in destabilization of the sol. Thus, the packing of solids within the template pores is likely to be significantly less than the maximum possible density. This could potentially lead to cracking and defects caused by the large volume change upon drying as the solvent is removed. In addition, the degree of shrinkage will be very high. This could lead to nanorods that may not have the shape and dimensions of the template pores, or are hollow tubes. Some of the difficulties inherent in sol–gel methods can be overcome by the use of electrophoresis. For instance, sol–gel electrophoresis has been shown an effective means of making thick films. These films often are of greater thickness, density, and quality than those formed traditionally by sol–gel methods (e.g., dip coating, spin coating) alone.[13–19]

[*] Prof. G. Z. Cao, S. J. Limmer, S. Seraji, Dr. Y. Wu, T. P. Chou, C. Nguyen
Department of Materials Science and Engineering
University of Washington
Seattle, WA 98195-2120 (USA)
E-mail: gzcao@u.washington.edu

[**] SJL thanks the Center for Nanotechnology at the University of Washington and the NSF IGERT fellowship for financial support.

  1616-301X/02/0101-0059 $ 17.50+.50/0

We have recently demonstrated a method for using sol–gel electrophoresis in the formation of a single composition of oxide nanorod.[20] In this paper, we present a systematic study on the growth of various oxide nanorods. We show that the sol–gel electrophoresis method is widely applicable, and can be used for the template growth of a number of different oxide nanorods. Titania (TiO_2), barium titanate ($BaTiO_3$), silica (SiO_2), strontium niobate ($Sr_2Nb_2O_7$), and lead zirconate titanate ($Pb(Zr_{0.52}Ti_{0.48})O_3$, PZT) nanorods are all discussed here.

2. Results

Figure 1 shows scanning electron microscopy (SEM) images of TiO_2 nanorods grown in a PC membrane with 200 nm diameter pores by sol–gel electrophoresis, and fired to 700 °C for 15 min. These nanorods have a uniform diameter throughout their entire length, with a surface that is smooth over much or all of the length. Comparing the various rods, one can see that they all have roughly the same length and diameter. The image also shows that the rods are arranged roughly parallel to one another over a broad area on the substrate. The diameter of the TiO_2 nanorods is estimated to be ~150 nm, which is approximately 25 % smaller than the membrane pore diameter. This size difference is most likely due to the volume shrinkage caused by densification during the heat treatment. Figure 1b also shows some broken rods, and it can be seen that these rods are solid and dense. This implies that the growth of the nanorods likely begins at the bottom of the pores, and proceeds from one side of the membrane to the other, as will be discussed in detail later in this paper. X-ray diffraction (XRD) spectra of the TiO_2 rods are shown in Figure 2, along with the spectra for a powder formed from the same sol and fired at 700 °C for 15 min. From the powder XRD spectrum, it can be seen that the sample consists of almost purely the anatase phase, with a small amount of rutile. Normally, the anatase phase converts to rutile upon heating at 700 °C,[21] which is the temperature to which these samples were heated. We believe that the incomplete conversion to rutile seen here may be due to a combination of factors. One is the short time (15 min) for which the rods were held at 700 °C, which may not have been sufficient to allow for complete transformation. In addition, the actual temperature that the samples experienced may have been somewhat less than 700 °C, due to fluctuations in the furnace. Lastly, it is possible that the particular sol-processing method used in this study is, in some way, responsible for this delayed conversion. Comparison of the two spectra shows that there are identical peaks in both samples. Further, the peak positions are the same and the intensity ratios among various peaks are similar. Note that there is a large amorphous background associated with the TiO_2 nanorods. This is due to the small amount of rods available for analysis, meaning that much of the X-ray beam was hitting the (amorphous) sample holder.

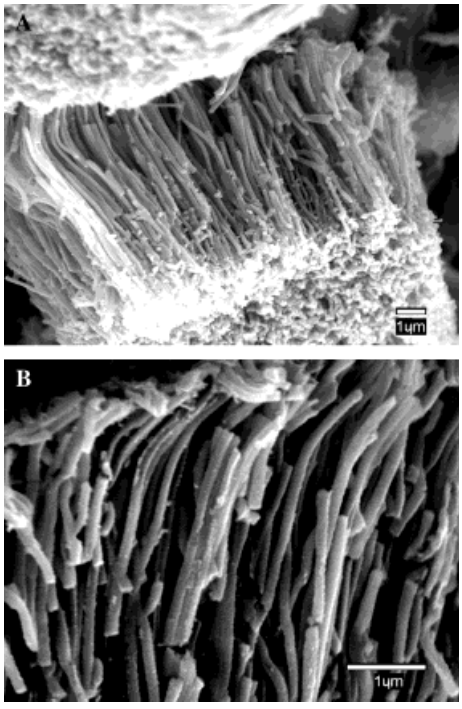

Fig. 1. SEM images of TiO_2 nanorods grown in a PC membrane with 200 nm diameter pores by sol–gel electrophoresis. A) Lower magnification image, showing that the rods are aligned and grown over a large area. B) Higher magnification image of the nanorods. Examination of the broken rods seen here shows that they are solid and dense.

Figures 3a–d show SEM images of $BaTiO_3$, SiO_2, $Sr_2Nb_2O_7$, and PZT nanorods, respectively, grown by sol–gel electrophoresis. The $BaTiO_3$ nanorods have a diameter of about 150 nm,

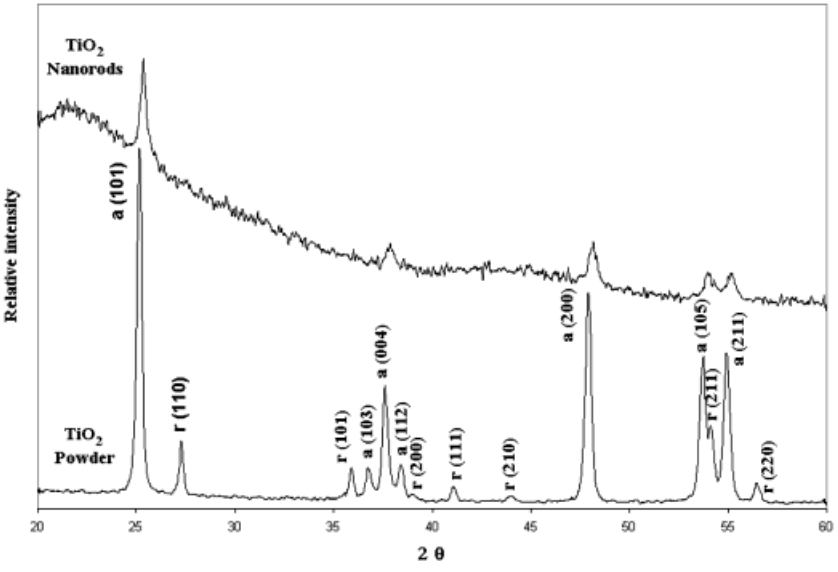

Fig. 2. XRD spectra of both the grown TiO_2 nanorods and a powder derived from the same sol. Both samples consist of largely the anatase phase, with some rutile present, and there is no observed shift in the peak positions for the nanorod sample. In addition, the relative intensities of the peaks are the same for the nanorod sample, showing that there is no preferred orientation in the sample. In the figure, "a" refers to the anatase phase, and "r" to the rutile phase.

1616-301X/02/0101-0060 $ 17.50+.50/0

ADVANCED FUNCTIONAL MATERIALS

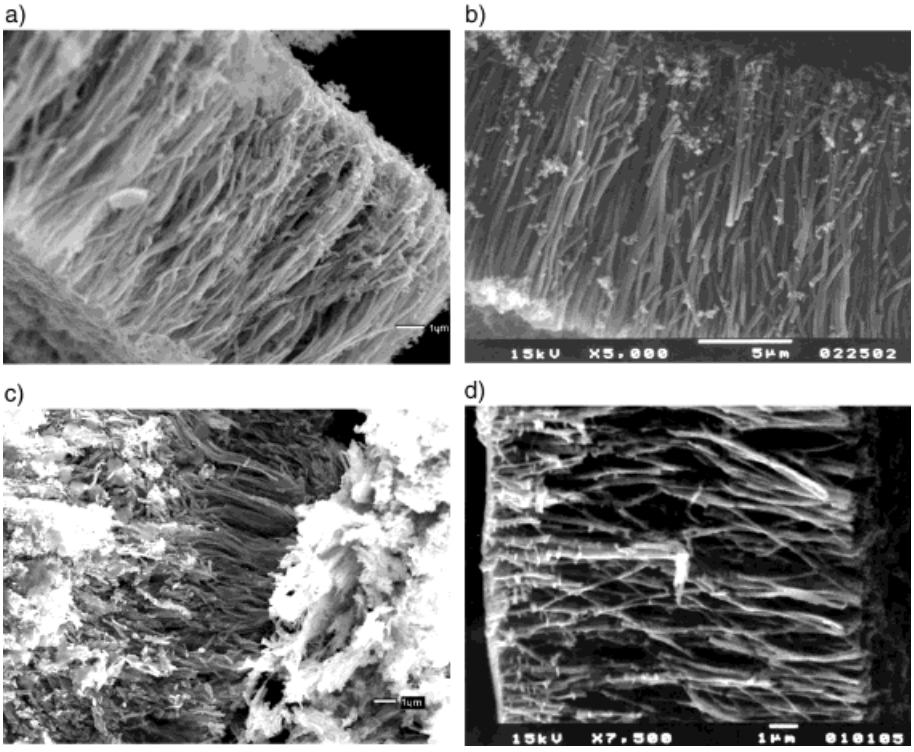

Fig. 3. SEM images of a) $BaTiO_3$, b) SiO_2, c) Sr_2-Nb_2O_7, and d) PZT nanorods grown in a PC membrane with 200 nm diameter pores by sol–gel electrophoresis.

which is about 25 % smaller than the template pores. The length of the $BaTiO_3$ rods is about 10 μm, similar to the thickness of the template membrane. The SiO_2 nanorods have a diameter of ~200 nm, which is the same as the template pores. Under the acidic synthesis conditions used, the silica sol should be polymeric.[22,23] Such a polymeric sol would pack very densely in the template pores, and the silica would thus contain only very small pores. This makes it likely that the SiO_2 nanorods were unable to densify significantly at the temperature used (500 °C). The $Sr_2Nb_2O_7$ and PZT nanorods have diameters of ~125 nm and ~150 nm, respectively. This corresponds to shrinkages of about 37 % and 25 % for these two materials, suggesting that $Sr_2Nb_2O_7$ did not pack as densely as the other materials. Similar to the TiO_2 nanorods, these nanorods also exhibit a uniform diameter throughout their entire length and have a relatively smooth surface. For each composition, the nanorods all have roughly the same length and diameter. These images also show that the rods are formed over a broad area on the surface, and are arranged roughly parallel to one another.

Also similar to the TiO_2 nanorods, the composition of a complex oxide formed by this technique (such as $Sr_2Nb_2O_7$) will consist of the desired crystalline phase with the desired stoichiometry. We have recently demonstrated this fact[20] for the complex oxide PZT. Figure 4 shows XRD spectra of the PZT nanorods and PZT powder prepared from the same sol; both PZT nanorods and powder consisted of only one crystalline phase, perovskite PZT, without any detectable secondary phase. Comparison of the two spectra shows that there are identical peaks in both samples. Further, the peak positions are the same and the intensity ratios among various peaks are identical. Similar XRD results were obtained when comparing $BaTiO_3$ powder and nanorods. This demonstrates that the electrophoretic deposition does not negatively affect the stoichiometry and chemical compositional homogeneity that is achieved during the sol preparation, and thus yields complex oxide rods of the desired phase and composition.

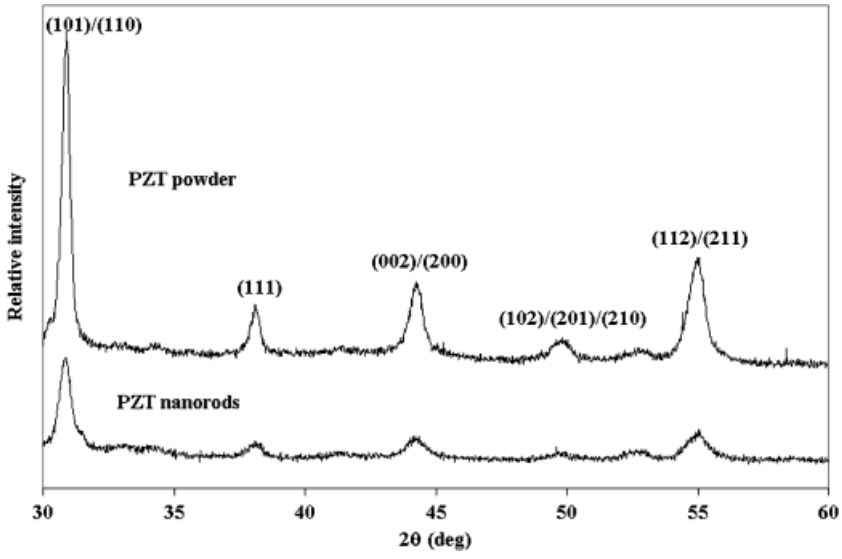

Fig. 4. XRD spectra of both the grown PZT nanorods and a powder derived from the same sol. Both samples show only a single perovskite phase. This demonstrates that sol–gel electrophoresis can be used to form complex oxides with the desired stoichiometry and crystal phase.

  1616-301X/02/0101-0061 $ 17.50+.50/0

3. Discussion

Few processing techniques have the flexibility inherent in sol–gel processing. An appropriate sol-preparation procedure yields solid nanoclusters with the desired stoichiometric chemical composition. These clusters are typically on the order of a few nanometers in size.[22] One of the advantages of sol–gel processing is that it allows the formation of compounds that have compositional homogeneity at a molecular level, which is very important for the formation of complex oxides. Sol–gel processing also offers many advantages for the processing of materials such as organic–inorganic hybrids, nanocomposites, and coatings on complex patterned surfaces. Another advantage of sol–gel processing is the stability conferred on many sols by electrostatic stabilization. That is, the nanoscale solid clusters that form in the sol are dispersed in a dilute electrolyte solvent. The surface of these nanoclusters becomes charged and counter ions in the solvent will distribute in such a way that an electrical double-layer at the vicinity of each nanocluster will be formed. This layer is due to a combination of electrostatic force, entropic force, and Brownian motion. Such an electrical double layer will keep the nanoclusters from agglomerating, and thus a stable sol is obtained. These charged nanoclusters have an oriented diffusion, parallel to the field direction, when an electric field is applied to the sol. In the present study, electrophoretic deposition was applied to grow nanorods of various oxides, capitalizing on the above advantages of sol–gel processing. Figure 5 is a schematic drawing of the electrophoretic deposition process. It demonstrates the steps we believe occur in the growth process. At the beginning of the nanorod growth, positively charged sol particles move due to electrophoresis towards the negative electrode. They deposit at the bottom of the pore, while the negatively charged counter ions move in the opposite direction. As time increases, the densely packed sol particles fill more of the pore, until the pore is completely filled. Dense cross-sections of TiO_2 nanorods observed by SEM and shown in Figure 1b suggest that the growth of oxide nanorods does indeed follow the mechanism proposed in Figure 5.

Under the experimental conditions applied in the current study, both the surface charge of the nanoclusters and the zeta-potential of the sol are either positive or negative, depending on the system. For the TiO_2 sol, the pH is about 2, well below the isoelectric point (6.2),[13] and thus the particles would be positively charged, and the zeta potential would also be positive in a dilute sol. For $BaTiO_3$, the pH is about 5, which also leads to positively charged particles and positive zeta potential. In the SiO_2 sol, the pH is about 3, which is just above the isoelectric point (~2), yielding negatively charged particles and a negative zeta potential. For PZT, since the pH of the sol (~4) is below the reported isoelectric point (~7.6),[24] the zeta potential is positive. In the case of the $Sr_2Nb_2O_7$ sol, no information about the isoelectric point of $Sr_2Nb_2O_7$ could be found in the literature. We assume that it contains positively charged particles at the given pH (~1), since oxide particles are often positively charged at such a low pH. The successful growth of $Sr_2Nb_2O_7$ nanorods demonstrates that this is a reasonable assumption.

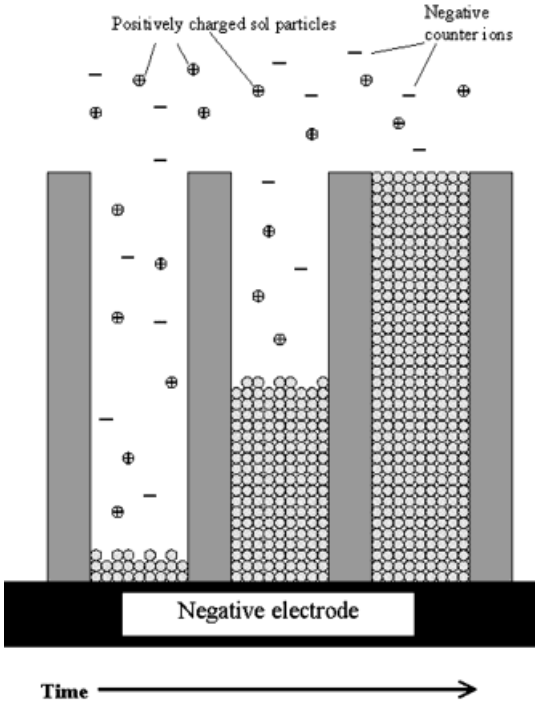

Fig. 5. This schematic demonstrates the progression of the growth process. At the left, we see the beginning of the nanorod growth. Positively charged sol particles are moving electrophoreticaly towards the negative electrode, depositing at the bottom of the pore, while the negatively charged counter ions are moving in the opposite direction. The center of the diagram shows a later time, as the densely packed sol particles fill more of the pore. Lastly, the right side of the diagram shows a completely filled pore.

Upon application of an appropriate potential, the charged nanoclusters dispersed in a solvent will be drawn towards the anode in the case of SiO_2, or the cathode in the case of the other oxides. The nanoclusters will fill the pores of the membrane from the bottom of the pores, where it is directly connected to the electrode. As the deposition proceeds, electrical conduction between the electrode and the growth surface would be accomplished by diffusion of counter-ions through the voids between packed nanoclusters. In this manner, all the pores will eventually be completely filled. Prolonged deposition times may lead to a thin layer of oxide forming on the membrane surface after the pores are filled. If we assume that the nanoclusters are uniformly sized spheres, then the highest possible packing density is 74 %.[25] This would also be the highest achievable density of the nanorods before densification. If there is a range of sizes in the nanoclusters, even denser packing could be possible. Upon heating the nanorods to an elevated temperature, densification will occur along with shrinkage. This explains why the observed diameter of the nanorods is smaller than that of the membrane pores. Although we do not know how closely the nanoclusters packed during the electrophoretic deposition, a lateral shrinkage of approximately 25–30 % was observed when the nanorods were fired. Since the times and temperatures used are sufficient to form fully dense films of these sols, it is reasonable to assume that the nanorods are also fully dense

  1616-301X/02/0101-0062 $ 17.50+.50/0

after firing. This in turn implies that near ideal close packing of nanoclusters might be achieved by this process.

The existence of broken nanorods in these figures could be explained as follows. The PC membrane templates burn off at approximately 400 °C in air, but the oxide nanorods are not likely to be fully dense (or crystallized) at this temperature, and thus have very limited mechanical strength. As the membrane and rods are heated, it is expected that some nanorods would break due to the differences in thermal expansion coefficients and distortion of the membranes.

4. Conclusions

In summary, we have demonstrated the applicability of sol–gel electrophoresis to the creation of various simple and complex oxide nanorods. Oxide nanorods with a diameter ~125–200 nm and a length of about 10 μm were grown in PC membranes using sol–gel electrophoresis. This technique offers several advantages, including the ability to grow large areas of uniformly sized and nearly unidirectionally aligned nanorods of various oxides. It is also believed to yield a more dense oxide nanorod prior to sintering than sol–gel without electrophoresis. Appropriate sol preparation can easily lead to formation of the desired stoichiometric chemical composition, which would be preserved during the electrophoretic growth of nanorods. Dense single-phase crystalline oxide nanorods can be readily obtained by firing at elevated temperatures.

5. Experimental

The chemicals used in making the sols were: titanium(IV) isopropoxide (97 %, Alfa Aesar, Ward Hill, MA), zirconium *n*-propoxide (70 % in propanol, Alfa Aesar, Ward Hill, MA), tetraethyl orthosilicate (98 %, Aldrich), lead(II) acetate (99 %, Alfa Aesar, Ward Hill, MA), barium acetate (Morton Thiokol, Danvers, MA), niobium pentachloride (99.8 %), and strontium nitrate (99 %, Aldrich). Hydrochloric acid (37.5 %, Fisher), glacial acetic acid (Fisher Scientific, Fair Lawn, NJ), lactic acid (Sigma Chemical, St. Louis, MO), ethylene glycol, glycerol (both J. T. Baker, Phillipsburg, NJ), and ethanol were also used. The template membranes used for the growth of the nanorods were track-etched hydrophilic PC (Millipore, Bedford, MA), with a pore diameter of 200 nm, and a thickness of 10 μm. An overview of the chemicals and conditions for the preparation of the various sols is given in Table 1.

TiO_2 sol was formed by first dissolving titanium(IV) isopropoxide in glacial acetic acid and stirring at 400 rpm for 30 min at room temperature. Deionized (DI) water was then added to the solution, and stirred for another 30 min. Upon addition of the water, a white precipitate instantaneously formed. However, the precipitate dissolved and the sol became a clear liquid after the first 5 min of stirring. Lactic acid, glycerol, and ethylene glycol were then added to form a sol that is stable at room temperature for about a week. The TiO_2 sol had a pH ~ 2.

$BaTiO_3$ sol was prepared by dissolving barium acetate in glacial acetic acid while stirring. This was done at room temperature, and the solution was stirred for about 30 min. To this solution, titanium(IV) isopropoxide was added, and the mixture was stirred for about 30 min. Lastly, ethylene glycol was added, and the sol was stirred at 90 °C for 1 h. The resultant sol was stable at room temperature for a period of months, and had a pH ≈ 5.

$Sr_2Nb_2O_7$ sol was prepared using the same procedure as reported in [26]. Ethanol and ethylene glycol were mixed and heated to 40 °C, followed by the addition of citric acid and strontium nitrate. This mixture was stirred for 150 min at 40 °C. The niobium pentachloride was then added, and the solution was stirred for another 90 min. During this time, water was slowly added to the mixture, forming the sol. The final concentration of this sol is about 0.6 M, and it is stable over a period of months at room temperature. The pH of the $Sr_2Nb_2O_7$ sol is ~1.

The SiO_2 sol was made by dissolving tetraethyl orthosilicate in a mixture of ethanol and DI water. A small amount of hydrochloric acid was added to the sol to adjust the pH to ~3 and the sol was stirred for 2 h at room temperature. The silica sol thus formed was rather stable, and took several weeks to gel at room temperature.

Table 1. An overview of the chemicals and conditions for the preparation of the various sols.

	Precursors	Solvents / Other chemicals	pH
TiO_2	Titanium (IV) isopropoxide	Glacial acetic acid, water, lactic acid, glycerol, ethylene glycol	~2
$BaTiO_3$	Titanium (IV) isopropoxide, barium acetate	Glacial acetic acid, ethylene glycol	~5
SiO_2	Tetraethyl orthosilicate	Ethanol, water, hydrochloric acid	~3
$SrNb_2O_6$	Strontium nitrate, niobium chloride	Ethylene glycol, ethanol, citric acid, water	~1
$Pb(Zr,Ti)O_3$	Lead (II) acetate, titanium isopropoxide, zirconium *n*-propoxide	Glacial acetic acid, water, lactic acid, glycerol, ethylene glycol	~4

The preparation of PZT sol was described in detail in [20]. Briefly, lead(II) acetate is dissolved in glacial acetic acid, and heated to 110 °C for ~15 min to dehydrate the lead acetate. The sample is then allowed to cool back to room temperature. Because of the volatility of PbO, an excess amount of lead (5 mol-%) is used in the fabrication of this sol. Then titanium(IV) isopropoxide and zirconium(IV) *n*-propoxide are mixed together for ~10 min at room temperature, and added to the lead solution once it has cooled to room temperature. Deionized water is then added to initiate and sustain hydrolysis and condensation reactions, and the sol is stirred for ~15 min at room temperature. Lastly, lactic acid, glycerol, and ethylene glycol are added to adjust the viscosity and stability of the sol. Such prepared sols have a concentration of about 5 vol.-% PZT, and are stable for several weeks at room temperature.

Nanorods of these oxides were formed by the following method. For all materials except SiO_2, an anode of Pt mesh is immersed in the sol, and the cathode used is aluminum. For SiO_2, the electrodes are reversed (Pt cathode, template on anode) since the SiO_2 particles are negatively charged. The PC membrane is attached to the electrode with a piece of double-sided conductive (carbon) tape, to provide a conductive path from the membrane to the cathode. This electrode is placed on top of and just in contact with the sol, and the sol is drawn into the membrane pores by capillary action, as shown schematically in Figure 6. For the electrophoretic growth, a potential of 5 V is applied between the electrodes, and held for up to 3 h. At the end of the electrophoretic deposition, excess sol is blotted off the membrane, and the membrane is then transferred from the electrode to a clean piece of Si wafer. Samples prepared in this manner are dried at ~100 °C for several hours, then placed in an oven and fired. The temperature for this firing is either 500 °C (SiO_2) or 700 °C (TiO_2, $BaTiO_3$, $Sr_2Nb_2O_7$, and PZT) for 15–30 min. This is to burn off the PC membranes, make the nanorods dense,

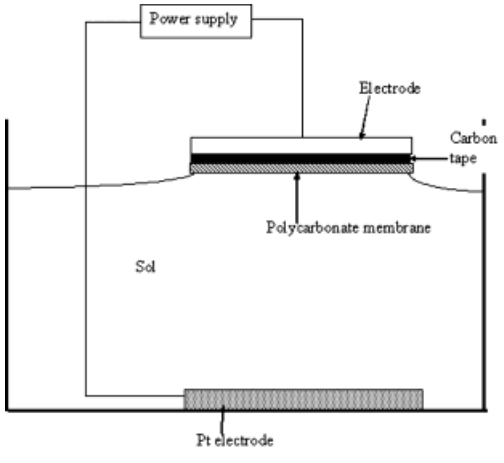

Fig. 6. Diagram of the experimental setup used for growth of nanowires by sol–gel electrophoresis. One electrode is a Pt mesh, and the other electrode is Al. The PC membrane is attached to the Al electrode with a piece of double-sided conductive (carbon) tape, to provide a conductive path. This electrode is placed on top of and just in contact with the sol, and the sol is drawn into the membrane pores by capillary action.

  1616-301X/02/0101-0063 $ 17.50+.50/0

and crystallize the material (for all but SiO_2). In order to study the morphology of the nanorods, SEM (JEOL JSM-5200 and JEOL 840A) was used. Samples were sputter-coated with a thin Au/Pd layer prior to observation in the SEM. For all samples that we expected to be crystalline (all except SiO_2), XRD (Phillips PW1830) was used to determine the phases and crystal structures present, and to check for the presence of texture and degree of crystallinity.

Received: May 8, 2001
Final version: July 31, 2001

[1] J. J. Ramsden, M. Grätzel, *J. Chem. Soc.* **1984**, *80*, 919.
[2] J. C. Hulteen, C. R. Martin, *J. Mater. Chem.* **1997**, *7*, 1075.
[3] J. Westwater, D. P. Gosain, S. Tomiya, S. Usui, H. Ruda, *J. Vac. Sci. Technol. B* **1997**, *15*, 554.
[4] X. Duan, C. M. Lieber, *Adv. Mater.* **2000**, *12*, 298.
[5] B. Gates, Y. Yin, Y. Xia, *J. Am. Chem. Soc.* **2000**, *122*, 12 582.
[6] Z. W. Pan, Z. R. Dai, Z. L. Wang, *Science* **2001**, *291*, 1947.
[7] A. Huczko, *Appl. Phys. A* **2000**, *70*, 365.
[8] L. Piraux, S. Dubois, S. Demoustier-Champagne, *Nucl. Instrum. Methods Phys. Res. B* **1997**, *131*, 357.
[9] C. Schönenberger, B. M. I. Van der Zande, L. G. J. Fokkink, M. Henry, C. Schmid, M. Krüger, A. Bachtold, R. Huber, H. Birk, U. Staufer, *J. Phys. Chem. B* **1997**, *101*, 5497.
[10] B. B. Lakshmi, C. J. Patrissi, C. R. Martin, *Chem. Mater.* **1997**, *9*, 2544.
[11] Y. Li, G. S. Cheng, L. D. Zhang, *J. Mater. Res.* **2000**, *15*, 2305.
[12] V. M. Cepak, J. C. Hulteen, G. Che, K. B. Jirage, B. B. Lakshmi, E. R. Fisher, C. R. Martin, *J. Mater. Res.* **1998**, *13*, 3070.
[13] H. Hirashima, Y. Obu, T. Nagai, H. Imai, *Mater. Res. Soc. Symp. Proc.* **1994**, *346*, 95.
[14] L. Shaw, R. Abbaschian, *J. Am. Ceram. Soc.* **1995**, *78*, 3376.
[15] H. Nishimori, K. Hasegawa, M. Tatsumisago, T. Minami, *J. Sol–Gel Sci. Technol.* **1996**, *7*, 211.
[16] H. Nishimori, M. Tatsumisago, T. Minami, *J. Mater. Sci.* **1996**, *31*, 6529.
[17] K. Hasegawa, H. Nishimori, M. Tatsumisago, T. Minami, *J. Mater. Sci.* **1998**, *33*, 1095.
[18] K. Katagiri, K. Hasegawa, A. Matsuda, M. Tatsumisago, T. Minami, *J. Am. Ceram. Soc.* **1998**, *81*, 2501.
[19] K. Hasegawa, S. Kunugi, M. Tatsumisago, T. Minami, *J. Sol–Gel Sci. Technol.* **1999**, *15*, 243.
[20] S. J. Limmer, S. Seraji, M. J. Forbess, Y. Wu, T. P. Chou, C. Nguyen, G. Z. Cao, *Adv. Mater.* **2001**, *13*, 1269.
[21] Y. Hamasaki, S. Ohkubo, K. Murakami, H. Sei, G. Nogami, *J. Electrochem. Soc.* **1994**, *141*, 660.
[22] C. J. Brinker, G. W. Scherer, *Sol–Gel Sciences*, Academic, San Diego, CA **1990**.
[23] C. M. Chan, G. Z. Cao, H. Fong, M. Sarikaya, T. Robinson, L. Nelson, *J. Mater. Res.* **2000**, *15*, 148.
[24] K. Baba, O. Nishizato, A. Takamura, M. Katsube, *J. Ceram. Soc. Jpn.* **1993**, *101*, 1370.
[25] J. S. Reed, *Principles of Ceramic Processing*, Wiley, New York **1995**.
[26] S. Seraji, Y. Wu, N. E. Jewell-Larson, M. J. Forbess, S. J. Limmer, T. P. Chou, G. Z. Cao, *Adv. Mater.* **2000**, *12*, 1421.

  1616-301X/02/0101-0064 $ 17.50+.50/0